2010 American Control Conference
Marriott Waterfront, Baltimore, MD, USA
June 30-July 02, 2010

Boundary Actuation Structure of Linearized Two-Phase Flow

S. Djordjevic, O.H. Bosgra, P.M.J. Van den Hof, D. Jeltsema

Abstract— **In this paper, we introduce a two-phase flow model which describes the motion of two incompressible fluids. The proposed model is governed by nonlinear partial differential algebraic equations (PDAEs) with open initial-boundary conditions. The well-posedness of the boundaries is analyzed using characteristic curves, which leads to development of a boundary actuation structure that is suitable for a control design. A particular emphasis is placed on a possible coordinate transformation that can reduce the problem to a set of partial differential equations (PDEs) without algebraic constraints. The boundary actuation strategy is presented using linearized model equations and tested on a numerical example for a quasi steady-state situation.**

I. Introduction

Two-phase flow is of great relevance for many industrial applications ranging from chemical industry to oil production, and nuclear engineering. It is generally understood as a simultaneous flow of two different phases which interact via an infinitesimal thin interface. In most cases, the phases are simply referred to as gas/vapor, liquid, or solid state. For a long time, the analysis of two-phase flow processes was limited to mostly empirical correlations, or to largely simplified engineering models [1], [2], [3]. In recent years, due to the wide range of applications, a large effort has been spent on analysis of fluid dynamics in two-phase systems, and on development of related numerical simulation methods [4], [5], [6]. The model equations for two-phase flow in the fluid dynamics approach are usually derived by averaging the equations describing the fluid dynamics of the single-phase flow and couple them via different interactive terms. The result of this approach is a set of equations having a similar structure as the single-phase flow (i.e., Navier-Stokes equations) from which they originated [7]. Many of the present advanced models use different interactive terms between the phases with specific physical background and closure equations [4]. The correct formulation of the basic two-phase flow models and the appropriate form of the closure laws have been widely discussed in the past [5], [8], and, up to now, a commonly agreed approach has not been achieved. A great concern has been that most models presently used in the Computational Fluid Dynamics (CFD) codes are based on governing equations with several coupling terms and ill-posed boundary conditions [6], [9]. In order to avoid this kind of ill-posedness, it is sufficient to consider a proper boundary and to enforce coupling terms. This means that by designing a well-posed boundary actuation strategy subject to the boundary input, the performances of two-phase flow can be significantly improved.

The boundary actuation strategy and control laws for fluid systems have received considerable attention over the last few years [10]. As an initial study for the introduction of control theory into the fluid mechanical setting, the linearized Navier-Stokes equations have been considered [11], [12], [13]. The linearized model equations govern small perturbations around laminar flow which can be influenced from the boundaries via different boundary control laws. Several boundary control approaches are presented [14], [15], [16], [17] in which the manipulated boundary actuation is used to stabilize/destabilize the flow. Although there is a number of complex issues underlying the fluid dynamics, the stabilization of laminar flow described by linearized Navier-Stokes equations shows a promising control design for practical applications of single-phase flow.

In this paper, our objective is to introduce the second phase in the fluid mechanical systems, and to develop a control-oriented model with a well-posed boundary actuation structure. Once the well-posed model is derived, the various type of boundary control laws can be designed. We present the actuation strategy for the linearized model equations as a starting point for designing a boundary control law. The linearization technique is similar to the linearization technique presented in [17]. We also introduce different coordinate transformations which eventually lead to a hyperbolic PDE model with decoupled directional derivatives [18], [19], and reduce the model complexity and simulation time.

The paper is organized as follows. First, the model of a one-dimensional two-phase flow is presented. Second, the well-posedness of the proposed model is studied. Further, the linearized model equations are presented, and finally the boundary actuation structure is introduced using different coordinate transformations and tested on a numerical example.

II. The Dynamical Model

We consider a one-dimensional incompressible two-phase flow in a vertical pipe with an interfacial pressure and a drag force as the coupling terms between the two phases: gas and liquid [9]. The proposed model equations can be written in a matrix form as

$$\mathbf{E}\frac{\partial \Phi}{\partial t} + \mathbf{A}(\Phi)\frac{\partial \Phi}{\partial x} = \mathbf{c}(\Phi), \tag{1}$$

where $\Phi = \begin{bmatrix} \alpha_g & v_g & v_l \end{bmatrix}^T$ is the vector of flowing variables, α_g is the volume fraction of the gas phase, v_g

This work is supported by the Delft Center for Sustainable Industrial Processes, The Netherlands

S. Djordjevic, O.H. Bosgra, and P.M.J. Van den Hof are with the Delft Center for Systems and Control, Delft University of Technology, Mekelweg 2, 2628 CD Delft, The Netherlands. s.djordjevic@tudelft.nl.

D. Jeltsema is with the Delft Institute of Applied Mathematics, Delft University of Technology, Mekelweg 4, 2628 CD Delft, The Netherlands.

is the velocity of the gas phase, and v_l is the velocity of the liquid phase. The matrices

$$\mathbf{E} = \begin{bmatrix} 1 & 0 & 0 \\ 0 & \rho_g & -\rho_l \\ 0 & 0 & 0 \end{bmatrix}, \tag{2}$$

and

$$\mathbf{A}(\Phi) = \begin{bmatrix} v_g & \alpha_g & 0 \\ C_p\,\rho_l\,(v_g - v_l)^2 & \rho_g v_g & -\rho_l v_l \\ v_g - v_l & \alpha_g & 1-\alpha_g \end{bmatrix}, \tag{3}$$

are the system matrices, and

$$\mathbf{c}(\Phi) = \begin{bmatrix} 0 \\ -(\rho_g - \rho_l)g - (v_g - v_l)\left(\frac{\beta}{\alpha_g} + \frac{\beta}{1-\alpha_g}\right) \\ 0 \end{bmatrix}, \tag{4}$$

is the coupling force vector, where ρ_g is the density of gas phase, ρ_l is the density of liquid phase, C_p is the interfacial pressure coefficient, and g is the gravitational acceleration. Since $\mathbf{E}$ is a singular matrix, the proposed model for two-phase flow is a partial differential algebraic equations (PDAEs) model. The drag force in $\mathbf{c}(\Phi)$ is defined by the following closure equation

$$\beta = \frac{3C_d}{4d_b}\alpha_g\alpha_l\rho_l|v_g - v_l|,$$

where C_d is the drag coefficient and d_b is the diameter of a single bubble (i.e., particle of a discrete phase). Most of the closure relations in fluid dynamics are of empirical nature or include some heuristic elements which can not be deduced completely from first principles. However, there is a common agreement that the pure transport of the governing system equations of two-phase flow should be of hyperbolic nature with real distinct eigenvalues [9].

The sum of the volume fractions of the gas and liquid phase in an observed volume equals one, i.e., $\alpha_g + \alpha_l = 1$. Thus, the volume fraction of the gas phase can range between $0 \leq \alpha_g \leq 1$. If $\alpha_g = 0$, then only the liquid phase is present, and if $\alpha_g = 1$, then only the gas phase is present. In these situations, the model equations are in agreement with the equations for the single-phase flow. For the model derivation, we refer to Appendix A.

III. Well-posedness of the Model

The nature of the solutions to (1) is basically characterized by a characteristic polynominal of the system matrices (2) and (3). For PDAE models, the characteristic polynomial is of lower order than the order of the system. This means that the eigenvalues corresponding to the algebraic part have infinite many solutions, and the eigenvalues with the finite solutions correspond to the dynamical part. For the model (1), the eigenvalue analysis shows that the system has one infinite eigenvalue and two finite eigenvalues which are solutions of the following characteristic polynomial

$$\det(\lambda\mathbf{E} - \mathbf{A}(\Phi)) = a_1\lambda^2 + a_2\lambda + a_3, \tag{5}$$

with

$$\begin{aligned} a_1 &= -\alpha_g\rho_l - \rho_g + \rho_g\alpha_g, \\ a_2 &= 2\,\rho_g v_g - 2\,v_g\rho_g\alpha_g + 2\,\alpha_g\rho_l v_l, \\ a_3 &= -C_p\,\rho_l\,(v_g - v_l)^2\,{\alpha_g}^2 \\ &\quad + \left(\rho_g {v_g}^2 - \rho_l {v_l}^2 + C_p\,\rho_l\,(v_g - v_l)^2\right)\alpha_g - \rho_g {v_g}^2. \end{aligned}$$

The discriminant of (5) is defined by

$$D_c = a_2^2 - 4a_1a_3. \tag{6}$$

If $D_c > 0$, then the system (1) is said to be hyperbolic. The eigenvalues of the hyperbolic equations are real and distinct. If $D_c = 0$, the system is parabolic with real repeated eigenvalues. If $D_c < 0$, the system is elliptic with complex eigenvalues. Elliptic systems are ill-posed, whereas parabolic and hyperbolic systems are well-posed with a stable and unique solution [8]. For defining a critical point between the possible solutions, we evaluate (6) as

$$D_c = D\left(1 - \left(\frac{\rho_l\alpha_g + \alpha_l\rho_g}{\rho_g}\right)Cp\right) \tag{7}$$

where $D = \alpha_g\rho_g\rho_l\,(v_g - v_l)^2\,(-1 + \alpha_g)$. Since $\alpha_g < 1$, for all values of v_g and v_l, then $D < 0$. This means that the well-posedness of the model equations strongly depends on the interfacial pressure coefficient C_p. The critical C_p, for which the discriminant $D_c = 0$ and the system is parabolic, can be obtained from the system parameters ρ_g and ρ_l, and the volume fraction α_g

$$C_p = \frac{\rho_g}{\alpha_g\rho_l + \rho_g\alpha_l}.$$

The interfacial pressure coefficient C_p for an air/water system is reported to be between 0.25 and 0.5 [9]. This assures the hyperbolic region for a wide range of gas fractions. The finite eigenvalues for the proposed model read as

$$\lambda_1(\Phi) = \frac{\alpha_g\rho_l v_l + \alpha_l\rho_g v_g}{\alpha_g\rho_l + \alpha_l\rho_g} + \sqrt{D_c}, \tag{8}$$

$$\lambda_2(\Phi) = \frac{\alpha_g\rho_l v_l + \alpha_l\rho_g v_g}{\alpha_g\rho_l + \alpha_l\rho_g} - \sqrt{D_c}, \tag{9}$$

which are the characteristic velocities of the gas/liquid system.

IV. Linearized Model

This section gives a short overview of the linearization of the model equations which are used for developing a well-posed actuation structure of the two-phase flow model. The same linearization technique is also used for deriving the linearized Navier-Stokes equations in [17].

Suppose that $\overline{\Phi}$ is a steady-state solution of (1) and Φ' is a small perturbation around it, then the flow variable Φ can be written as

$$\Phi = \overline{\Phi} + \Phi', \tag{10}$$

and linearized system is given as (details of the derivation can be found in Appendix B)

$$\mathbf{E}\frac{\partial \Phi'}{\partial t} + \mathbf{A}(\overline{\Phi})\frac{\partial \Phi'}{\partial x} + \mathbf{A}(\Phi')\frac{\partial \overline{\Phi}}{\partial x} = \mathbf{F}\Phi', \qquad (11)$$

with

$$\mathbf{A}(\overline{\Phi}) = \begin{bmatrix} \overline{v_g} & \overline{\alpha_g} & 0 \\ C_p\,\rho_l\,(\overline{v_g} - \overline{v_l})^2 & \rho_g \overline{v_g} & -\rho_l \overline{v_l} \\ \overline{v_g} - \overline{v_l} & \overline{\alpha_g} & 1 - \overline{\alpha_g} \end{bmatrix},$$

$$\mathbf{A}(\Phi') = \begin{bmatrix} {v_g}' & {\alpha_g}' & 0 \\ 2\,C_p\,\rho_l\,(\overline{v_g} - \overline{v_l})\,({v_g}' - {v_l}') & \rho_g {v_g}' & -\rho_l {v_l}' \\ v_g' - v_l' & {\alpha_g}' & -{\alpha_g}' \end{bmatrix},$$

and

$$\mathbf{c}(\Phi') = \begin{bmatrix} 0 \\ 2\frac{3}{4}\frac{C_d}{d_b}\rho_l\,(\overline{v_g} - \overline{v_l})\,({v_g}' - {v_l}') \\ 0 \end{bmatrix}.$$

Equation (11) represents the linearized model where the steady-state solution can vary with respect to space according to $\frac{\partial \overline{\Phi}}{\partial x}$. If there is no variation with respect to space, i.e., $\overline{\Phi} = \text{const}$, the linearized model reduces to

$$\mathbf{E}\frac{\partial \Phi'}{\partial t} + \mathbf{A}(\overline{\Phi})\frac{\partial \Phi'}{\partial x} = \mathbf{F}\Phi'. \qquad (12)$$

A. Operational Regimes

In general, a steady-state solution is obtained by setting time derivatives of Φ to zero. For the proposed model, the steady-state solution can be obtained from

$$\mathbf{A}(\Phi)\frac{\partial \Phi}{\partial x} = \mathbf{c}(\Phi)$$

for the heterogeneous steady-state regime where the solutions can vary with respect to space. For the homogeneous regime, the gas distribution is a constant value, and the steady-state solution can be obtained from $\mathbf{c}(\Phi) = 0$. We refer to this situation as a quasi steady-state solution. If we compare this result with (17) and (18) (see Appendix A), we can recover the pressure in the steadiness as

$$\frac{dp}{dx} = -(\alpha_g \rho_g + \alpha_l \rho_l) g.$$

As can be expected, the pressure in the homogeneous steadiness is equal to hydrostatic pressure which gives a physical interpretation of the quasi steady-state solution. This means that in the homogeneous steadiness the gravity and the drag force are in balance. In order to predict the velocities in the quasi steady-state, we introduce a slip velocity v_s as a difference between the velocity of the gas phase and the velocity of the liquid phase [9]

$$v_s = v_g - v_l = \sqrt{\frac{4}{3}\frac{(\rho_l - \rho_g) g d_b}{C_d \rho_l}}.$$

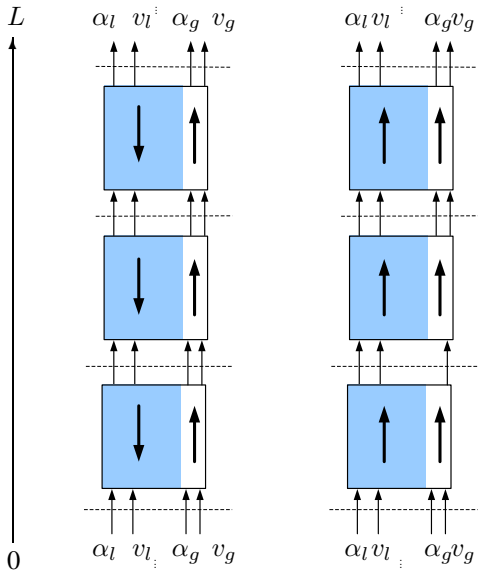

Fig. 1. Operational regimes: counter-current flow (left) and co-current flow (right).

Due to the compensating volumetric fluxes across an observed volume $\alpha_g v_g + \alpha_l v_l = 0$, the velocities in the homogeneous steady-state equal $v_g = \alpha_l v_s$ and $v_l = -\alpha_g v_s$. Depending on the flow direction, the liquid velocity can have a positive or a negative sign, which leads to different flow regimes. Fig. 1 illustrates two extreme regimes: counter-current and co-current regime in a vertical column divided on a few macroscopic observation volumes. In principle, for a real flow, there is a certain amount of fluids moving downwards and certain amount that moves upwards. This circulation phenomena for the one-dimensional flow is a sum of the upwards and downwards flow. Which flow is dominant depends on the gas and liquid injection and boundary actuation. In the following section, we describe the use of these equations for a control purpose.

B. Boundary Actuation

The behavior of hyperbolic-like equations is usually described as a wave propagation with the speed defined by characteristic velocity. The fundamental idea associated with the wave propagation is the notion of characteristic curves in the space-time domain along which these waves propagate. Using the linearized model (12), we can set

$$\mathbf{E}\frac{d\Phi'}{dt} = \mathbf{c}(\Phi') \quad \text{along the curves of} \quad \mathbf{E}\frac{dx}{dt} = \mathbf{A}(\overline{\Phi}).$$

The physical interpretation of the characteristic curves analysis is rather straightforward. The wave speeds of the propagation correspond to the characteristic velocities $\lambda_1(\overline{\Phi})$ and $\lambda_2(\overline{\Phi})$, and carry the gas fraction of phases injected at the boundaries. When we inject the gas/liquid phase at inlet/outlet, the phases will propagate upwards or downwards according to the sign of $\lambda_1(\overline{\Phi})$ and $\lambda_2(\overline{\Phi})$. If we have $0 < \lambda_1(\overline{\Phi}) < \lambda_2(\overline{\Phi})$, then both characteristic families of curves propagate as $\xi_1 = x - \lambda_1(\overline{\Phi})t$ and $\xi_2 = x - \lambda_2(\overline{\Phi})t$ in (x, t) plane [18], [19]. This means that the boundary

conditions must be specified at $\Phi'(t,0)$. However, if the eigenvalues are negative, the characteristic curves are defined as $\xi_1 = x_1 + \lambda_1(\overline{\Phi})t$ and $\xi_2 = x_2 + \lambda_2(\overline{\Phi})t$, and the boundary conditions must be defined at $\Phi'(t,L)$. It is rather common to have positive and negative eigenvalues, where for the positive eigenvalues the boundary conditions have to be specified at $\Phi'(t,0)$, whereas for the negative eigenvalues the boundary conditions should be specified at $\Phi'(t,L)$. As can be seen, the directional derivatives correspond to the eigenvalues of $(\mathbf{A}(\overline{\Phi}), \mathbf{E})$ along the characteristic curves defined by two ordinary differential equations

$$\frac{d\xi_1}{dt} = \lambda_1(\overline{\Phi}), \quad \text{and} \quad \frac{d\xi_2}{dt} = \lambda_2(\overline{\Phi}).$$

Since we deal with a PDAE model, i.e., a descriptor system along the characteristic curves, we introduce similarity transformation that eliminates the algebraic part of the model equations and decouple the wave velocities.

C. Coordinate Transformations

We use a standard coordinate transformation to rewrite the original linearized PDAE (12) as a linear PDE problem that involves only the dynamical part of the system. The system matrix $\mathbf{E}$ is diagonalized, so that in the new coordinates the linearized model can be reduced for the algebraic equation

$$\mathbf{E}^D = \mathbf{ET} = \begin{bmatrix} 1 & 0 & 0 \\ 0 & 1 & 0 \\ 0 & 0 & 0 \end{bmatrix}, \quad \mathbf{T} = \begin{bmatrix} 1 & 0 & 0 \\ 0 & {\rho_g}^{-1} & \rho_l \\ 0 & 0 & \rho_g \end{bmatrix}.$$

With $\mathbf{T}$ being the coordinate transformation matrix, we can transform the state Φ' into Ψ'

$$\Psi' = \begin{bmatrix} \alpha_g' \\ \rho_g v_g' - \rho_l v_l' \\ \dfrac{v_l'}{\rho_g} \end{bmatrix},$$

where $\Phi' = \mathbf{T}\Psi'$. This transformation allows the elimination of the algebraic part of PDAE in (12) which leads to a set of PDEs.In order to demonstrate the ability of the boundary actuation in enforcing well-posedness of the problem statement, simulations are carried out using a spatially uniformed steady-state solution (i.e., quasi steady-state regime) as an equilibrium point for the linearization. The algebraic equation in the new coordinates corresponds to $\dfrac{\partial \bar{\Psi}}{\partial t} = 0$ according to the matrix $\mathbf{E}^D$, and the model in the new coordinates can be written as

$$\mathbf{ET}\frac{\partial \Psi'}{\partial t} + \mathbf{A}(\overline{\Psi})\mathbf{T}\frac{\partial \Psi'}{\partial x} = \mathbf{FT}\Psi'. \tag{13}$$

After the elimination of the algebraic equation, the directional derivatives of the resulting set of PDEs can be further decoupled by diagonalizing $\mathbf{A}(\overline{\Psi})T$ in (13)

$$\frac{\partial}{\partial t}\begin{bmatrix} W_1' \\ W_2' \end{bmatrix} + \begin{bmatrix} \lambda_1 & 0 \\ 0 & \lambda_2 \end{bmatrix}\frac{\partial}{\partial x}\begin{bmatrix} W_1' \\ W_2' \end{bmatrix} = \begin{bmatrix} c_{11} & c_{12} \\ c_{21} & c_{22} \end{bmatrix}\begin{bmatrix} W_1' \\ W_2' \end{bmatrix}. \tag{14}$$

Equation (14) describes a linearized system of PDEs with decoupled wave propagation. The two solutions $W_1'(t,x)$ and $W_2'(t,x)$ are constant along the characteristic lines λ_1 and λ_2. Now, the boundary actuation strategy can be fully determined by the sign of the eigenvalues. The top boundary actuation $W'(t,L)$ of the linearized model is required for $\lambda < 0$, whereas the bottom boundary actuation $W'(t,0)$ is required for $\lambda > 0$. The equations are coupled according to the right-hand side of (14). The following numerical example shows the proposed boundary actuation strategy and stability analysis of the linearized system equations.

V. Numerical Example

In this section, we consider a numerical example for the linearized model equations around the previously described quasi steady-state solution. The fluid properties and the parameter values are given in Table I. The flow variables in the quasi steady-state are obtained from the constant gas distribution in the entire space divided into $N = 10$ observed volumes. For the constant gas fraction $\overline{\alpha_g} = 0.1$, the slip velocity is $v_s = 0.17$, the gas velocity is $\overline{v_g} = 0.155$, and the liquid velocity $\overline{v_l} = -0.017$. According to the sign of the steady velocities, the phases move in the opposite direction (see Fig.1 counter-current flow).

TABLE I
FLUID PROPERTIES AND SYSTEM PARAMETERS.

Symbol	Value	Unit
ρ_g	1	[kg/m^3]
ρ_l	1000	[kg/m^3]
C_d	0.440	[-]
d_b	0.001	[m]
C_p	1/4	[-]
g	9.81	[m/s^2]

For the given quasi steady-state situation, the eigenvalues are $\lambda_1 = 0.0954$, and $\lambda_2 = -0.064$. According to (14) and the boundary actuation strategy for the given system, the boundary condition for λ_1 has to be defined at the inlet, i.e., $W_1'(t,0)$, and the boundary condition for λ_2 has to be defined at the outlet, i.e., $W_2'(t,L)$. Fig. 2 and Fig. 3 illustrate the wave propagation of the characteristic solutions from the boundaries without force term, i.e., right-hand side of (14) equals zero. The simulation results clearly show the wave propagations and the stability of the solution $W_1'(t,x)$ and $W_2'(t,x)$, respectively. For the given boundary structure, the linearized system without force term is stable viewed as perturbations around the operating point. Fig. 2 and Fig. 3 show typical behavior of open conservative systems, i.e., first order hyperbolic systems.

On the other hand, Fig. 4 and Fig. 5 show the effect of the force term on the wave propagation as it is given in (14). For the wave that propagates from bottom to top, the effect of drag force is observed mostly at the top boundary caused by $c_{11}W_1'$ and $c_{12}W_2'$ with minor oscillation with respect to space (Fig. 4). The drag force has much stronger effect on the wave that propagates from the top. The deviations

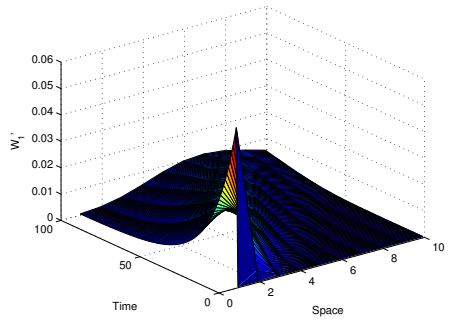

Fig. 2. Wave propagation of $W_1'(t,x)$ with speed λ_1 without forcing term $c_{11}W_1' + c_{12}W_2'$.

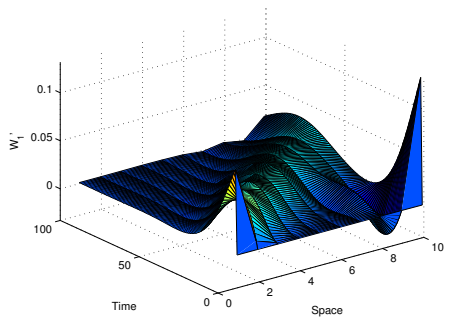

Fig. 4. Wave propagation of $W_1'(t,x)$ with speed λ_1 forced by $c_{11}W_1' + c_{12}W_2'$.

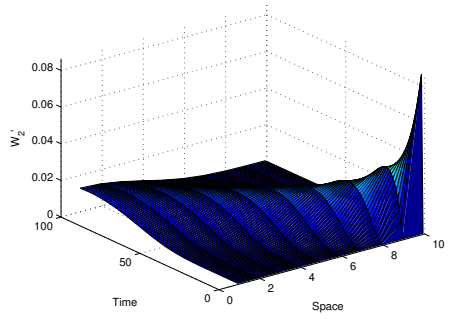

Fig. 3. Wave propagation of $W_2'(t,x)$ with speed λ_2 without forcing term $c_{21}W_1' + c_{22}W_2'$.

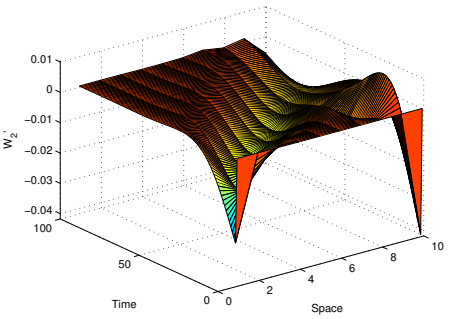

Fig. 5. Wave propagation of $W_2'(t,x)$ with speed λ_2 forced by $c_{21}W_1' + c_{22}W_2'$.

from the quasi-steady state occur as negative values in the defined solution domain. The sign of the eigenvalues and the coupling terms plays an important role in the stability analysis. Since $c_{12} > c_{11} > 0$ and $c_{11} = -c_{21}$ whereas $c_{12} = -c_{22}$, the stability of the wave which propagates with velocity λ_2 is largely influenced by c_{22}. This explains the oscillations in the solution W_2', as presented in Fig. 5. Although the system is stable, the wave velocities are rather influenced by the force coefficients c_{11}, c_{12}, c_{21}, and c_{22}. This means that by introducing more coupling terms on the right-hand side in (14) or by increasing the magnitude of the coefficients, the system will become unstable.

VI. Conclusions and Future Works

This paper introduces a linearized two-phase flow model and a structural analysis of the boundary actuation. The actuation strategy is based on decoupling the wave propagation of the linearized model using a coordinate transformation. The main contribution of this paper is to present a control-oriented model of two-phase flow with a well-posed boundary control strategy that reduces the computational complexity and enables the application of the advanced controllers. It is important to point out that, at the moment, the area of control of hydrodynamics of two-phase and multiphase flow is still an open control question, mainly due to the complex mathematical models behind the CFD codes.

References

[1] K.B. Bischoff and O. Levenspiel, Fluid dispersion-generalization and comparison of mathematical models. I. Generalization of models, *Chemical Engineering Science*, vol. 17,1962, pp 245–255

[2] S. Degaleesanm, S. Roy, S. B. Kumar and M. P. Duduković, Liquid mixing based on convection and turbulent dispersion in bubble columns, *Chemical Engineering Science*, vol. 51, 1996, pp 1967–1976

[3] S. Degaleesan, M.P. Dudukovic, B.A. Toseland and B.L. Bhatt , A Two-Compartment Convective-Diffusion Model for Slurry Bubble Column Reactors, *Industrial and Engineering Chemistry Research*, vol. 36, 1997, pp 4670–4680

[4] J. Joshi, Computational flow modelling and design of bubble column reactors *Chemical Engineering Science*, vol. 56, 2001, pp 5893-5933

[5] M. Ishii and T. Hibiki, *Thermo-fluid dynamics of two-phase flow*, Springer, 2006

[6] H. Stadtke *Gasdynamic Aspects of Two-phase Flow : Hyperbolicity, Wave Propagation Phenomena, and Related Numerical Methods*, Wiley-VCH, 2006

[7] D.A. Drew, Mathematical modeling of two-phase flow, *Annual review of fluid mechanics*, vol. 15, 1983, pp 261–291

[8] V. Ransom and D. Hicks, Hyperbolic two-pressure models for two-phase flow *Journal of Computational Physics*, vol. 53, 1984, pp 124-151

[9] J. Park, D. Drew and R. Lahey, Jr, The analysis of void wave propagation in adiabatic monodispersed bubbly two-phase flows using an ensemble-averaged two-fluid model, *International Journal of Multiphase Flow*, 1999, pp 1205-1244

[10] T.R. Bewley, Flow control: new challenges for a new Renaissance, *Progress in Aerospace Sciences*, vol. 37, 2001, pp 21-58

[11] S.S. Joshi, J.L. Speyer and J. Kim, A systems theory approach to the feedback stabilization of infinitesimal and finite-amplitude disturbances in plane Poiseuille flow, *Journal of Fluid Mechanics*, vol. 332, 1997, pp 157-184.

[12] S.S. Joshi, J.L. Speyer and J. Kim, Finite-dimensional optimal control of poiseuille flow, *Journal of Guidance, Control, and Dynamics*, vol. 22, 1999, pp 340-348
[13] L. Cortelezzi and J.L. Speyer, Robust reduced-order controller of laminar boundary layer transitions, *Phisical Review E*, vol. 58, 1998
[14] S.M. Kang, V. Ryder, L. Cortelezzi and J.L. Speyer, State-space formulation and controller design for three-dimensional channel flows, *Proceedings of the 1999 American Control Conference, San Diego, California*, 1999
[15] M.R. Jovanovic and B. Bamieh, Frequency domain analysis of the linearized Navier-Stokes equations, *Proceedings of the 2003 American Control Conference, Denver, Colorado*, 2003
[16] T.R. Bewley, P. Moin and R. Temam, DNS-based predictive control of turbulence: an optimal benchmark for feedback algorithms, *Journal of Fluid Mechanics*, vol. 447, 2001, pp 179-225
[17] O.M. Aamo and M. Krstic, *Flow control by feedback*, Springer; 2003
[18] J-M. Coron, J de Halleux and G. Bastin and B. d'Andrea-Novel, On boundary control design for quasilinear hyperbolic systems with entropies as Lyapunov functions, *IEEE Conference on Decision and Control*, 2002
[19] G. Bastin, J-M. Coron and B. dAndrea-Novel, Boundary feedback control and Lyapunov stability analysis for physical networks of 2 × 2 hyperbolic balance laws, *IEEE Conference on Decision and Control*, 2008

APPENDIX A

The two phase flow is described by instantaneous changes of mass and momentum of each phases involved. For the one-dimensional flow, the equations read

$$\frac{\partial \alpha_g}{\partial t} + \frac{\partial \alpha_g}{\partial x} v_g + \alpha_g \frac{\partial v_g}{\partial x} = 0, \tag{15}$$

$$\frac{\partial \alpha_l}{\partial t} + \frac{\partial \alpha_l}{\partial x} v_l + \alpha_l \frac{\partial v_l}{\partial x} = 0, \tag{16}$$

$$\alpha_g \rho_g \frac{\partial v_g}{\partial t} + \alpha_g v_g \rho_g \frac{\partial v_g}{\partial x} + \alpha_g \frac{dp}{dx} + \triangle p_g \frac{\partial \alpha_g}{\partial x} = - \alpha_g \rho_g g - \beta \left(v_g - v_l \right), \tag{17}$$

$$\alpha_l \rho_l \frac{\partial v_l}{\partial t} + \alpha_l v_l \rho_l \frac{\partial v_l}{\partial x} + \alpha_l \frac{dp}{dx} + \triangle p_l \frac{\partial \alpha_g}{\partial x} = - \alpha_l \rho_l g + \beta \left(v_g - v_l \right). \tag{18}$$

In (17) and (18), the pressure effect is modeled as a sum of two pressures: bulk pressure and interfacial pressure. For gas/liquid systems, the pressure difference within the gas phase is extremely small due to the low density of the gas phase, $\triangle p_g \approx 0$, whereas the pressure difference within the liquid phase can be estimated $\triangle p_l = C_p \alpha_l \rho_l (v_g - v_l)^2$ [9], [4], [8]. In order to eliminate the pressure gradient, we divide (17) and (18) by α_g and α_l respectively, and subtract one from the other. This step simplifies the model equations with respect to the implicitly modeled pressure. Furthermore, the model can be rewritten with respect to the gas volume fraction only by using the constraint, $\alpha_g + \alpha_l = 1$. After these simplification steps, the final form of the model can be written as

$$\frac{\partial \alpha_g}{\partial t} + \frac{\partial \alpha_g}{\partial x} v_g + \alpha_g \frac{\partial v_g}{\partial x} = 0, \tag{19}$$

$$\rho_g \frac{\partial v_g}{\partial t} - \rho_l \frac{\partial v_l}{\partial t} + \rho_g v_g \frac{\partial v_g}{\partial x} - \rho_l v_l \frac{\partial v_l}{\partial x} + C_p \rho_l (v_g - v_l)^2 \frac{\partial \alpha_g}{\partial x} = - (\rho_g - \rho_l) g - (v_g - v_l) \left(\frac{\beta}{\alpha_g} + \frac{\beta}{\alpha_l} \right), \tag{20}$$

$$\frac{\partial \alpha_g}{\partial x} (v_g - v_l) + \frac{\partial v_g}{\partial x} \alpha_g + (1 - \alpha_g) \frac{\partial v_l}{\partial x} = 0. \tag{21}$$

APPENDIX B

Inserting (10) into (1) for each equation separately, we obtain the linearized model using Taylor series. The linearized mass balance equation reads as

$$\frac{\partial \alpha_g'}{\partial t} + \frac{\partial \alpha_g'}{\partial x} \overline{v_g} + \overline{\alpha_g} \frac{\partial v_g'}{\partial x} + \frac{\partial \overline{\alpha_g}}{\partial x} v_g' + \alpha_g' \frac{\partial \overline{v_g}}{\partial x} = 0, \tag{22}$$

with $\alpha_g' \dfrac{\partial \alpha_g'}{\partial x} \approx 0$ for the perturbation in the vicinity of the steady-state solution. The linearized momentum equation is more computationally involved due to the nonlinear interfacial pressure and the drag force, i.e.,

$$\rho_g \frac{\partial v_g'}{\partial t} - \rho_l \frac{\partial v_l'}{\partial t} + \rho_g \overline{v_g} \frac{\partial v_g'}{\partial x} + \rho_g v_g' \frac{\partial \overline{v_g}}{\partial x} - \rho_l \overline{v_l} \frac{\partial v_l'}{\partial x} + C_p \rho_l \left(\overline{v_g} - \overline{v_l} \right)^2 \frac{\partial \alpha_g'}{\partial x} + 2 C_p \rho_l (\overline{v_g} - \overline{v_l}) \left(v_g' - v_l' \right) \frac{\partial \overline{\alpha_g}}{\partial x} - \rho_l v_l' \frac{\partial \overline{v_l}}{\partial x} = -2 \frac{3}{4} \frac{C_d}{d_b} \sqrt{(\overline{v_g} - \overline{v_l})^2} \left(v_g' - v_l' \right), \tag{23}$$

where $\left(v_g' - v_l' \right)^2 \frac{\partial \alpha_g'}{\partial x} \approx 0$, $\left(v_g' - v_l' \right) \frac{\partial \alpha_g'}{\partial x} \approx 0$, and $\left(v_g' - v_l' \right)^2 \approx 0$. The linearized algebraic equation equals

$$\frac{\partial \overline{\alpha_g}}{\partial x} (v_g' - v_l') + \frac{\partial \alpha_g'}{\partial x} (\overline{v_g} - \overline{v_l'}) + \frac{\partial \overline{v_g}}{\partial x} \alpha_g' + \frac{\partial v_g'}{\partial x} \overline{\alpha_g} + (1 - \overline{\alpha_g}) \frac{\partial v_l'}{\partial x} - \alpha_g' \frac{\partial \overline{v_l}}{\partial x} = 0. \tag{24}$$

Finally, the equations are given in the compact form (11).